

# Results from the TOM3 Testbed: Thermal Deformation of Optics at the Picometer Level.

R. Goullioud, C. A. Lindensmith, I. Hahn,  
Jet Propulsion Laboratory, California Institute of Technology,  
4800 Oak Grove Dr, M/S 171-113  
Pasadena, CA 91109  
818 354 7908  
renaud@jpl.nasa.gov

*Abstract*—Future space-based optical interferometers, such as the Space Interferometer Mission (SIM), require thermal stability of the optical wavefront to the level of picometers in order to produce astrometric data at the micro-arc-second level. In SIM, the internal path of the interferometer will be measured with a small metrology beam whereas the starlight fringe position is estimated from a large concentric annular beam. To achieve the micro-arc-second observation goal for SIM, it is necessary to maintain the optical path difference between the central and the outer annulus portions of the wavefront of the front-end telescope optics to a few tens of picometers for an hour.

The Thermo-Opto-Mechanical testbed (TOM3) was developed at the Jet Propulsion Laboratory to measure thermally induced optical deformations of a full-size flight-like beam compressor and siderostat, the two largest optics on SIM, in flight-like thermal environments. A Common Path Heterodyne Interferometer (COPHI) developed at JPL was used for the fine optical path difference measurement as the metrology sensor. The system was integrated inside a large vacuum chamber in order to mitigate the atmospheric and thermal disturbances. The Siderostat was installed in a temperature-controlled thermal shroud inside the vacuum chamber, creating a flight-like thermal environment. Detailed thermal and structural models of the test articles (siderostat and compressor) were also developed for model prediction and correlation of the thermal deformations. Experimental data shows SIM required thermal stability of the test articles and good agreement with the model predictions.

## TABLE OF CONTENTS

<b>1. INTRODUCTION</b>	<b>1</b>
<b>2. COMMON-PATH HETERODYNE INTERFEROMETER</b>	<b>3</b>
<b>3. TEST ARTICLES</b>	<b>5</b>
<b>4. THERMAL SYSTEM</b>	<b>6</b>
<b>5. TEST RESULTS</b>	<b>8</b>

<b>6. CONCLUSION</b>	<b>11</b>
<b>ACKNOWLEDGEMENTS</b>	<b>11</b>
<b>REFERENCES</b>	<b>11</b>
<b>BIOGRAPHY</b>	<b>11</b>

## 1. INTRODUCTION

The TOM3 experiment is a key ground-based testbed that demonstrates critical technologies for SIM, a space-based Michelson interferometer that will carry out astrometry to micro-arcsecond precision on the visible light from a large sample of stars in our galaxy. Detail discussion regarding SIM was addressed by Marr [1].

SIM has many technological challenges to address in order to show the mission is technically achievable. These challenges range from nanometer-level control problems to picometer-level sensing problems [2]. Several testbeds have been designed, built, and tested thus far in SIM's evolution. Each testbed is intended to resolve a system-level aspect of the SIM technology challenge. Examples of such testbeds include the SIM System Test-Bed 3 [3], Micro-Arcsecond Metrology testbed [4],[5], and the Kite testbed [6]. The results from these series of testbeds form the evidence that the technological challenges faced by SIM are achievable.

Interferometry of such high precision requires extremely accurate knowledge of optical path length difference (OPD) changes, hence precise internal metrology, which is to be carried out with laser heterodyne metrology gauges. For SIM to succeed, the optical path length metric provided by the interferometer fringe determination must be consistent, at the level of tens of picometers, with the distances measured by metrology gauges, under the flight-like thermal environment. The purpose of TOM3 testbed is to demonstrate this agreement in a full-scale simulation that implements the front-end fraction of the final SIM flight functionality.

<sup>1</sup> 0-7803-9546-8/06/\$20.00© 2006 IEEE

<sup>2</sup> IEEEAC paper #1422, Version 2, Updated December 19, 2005.

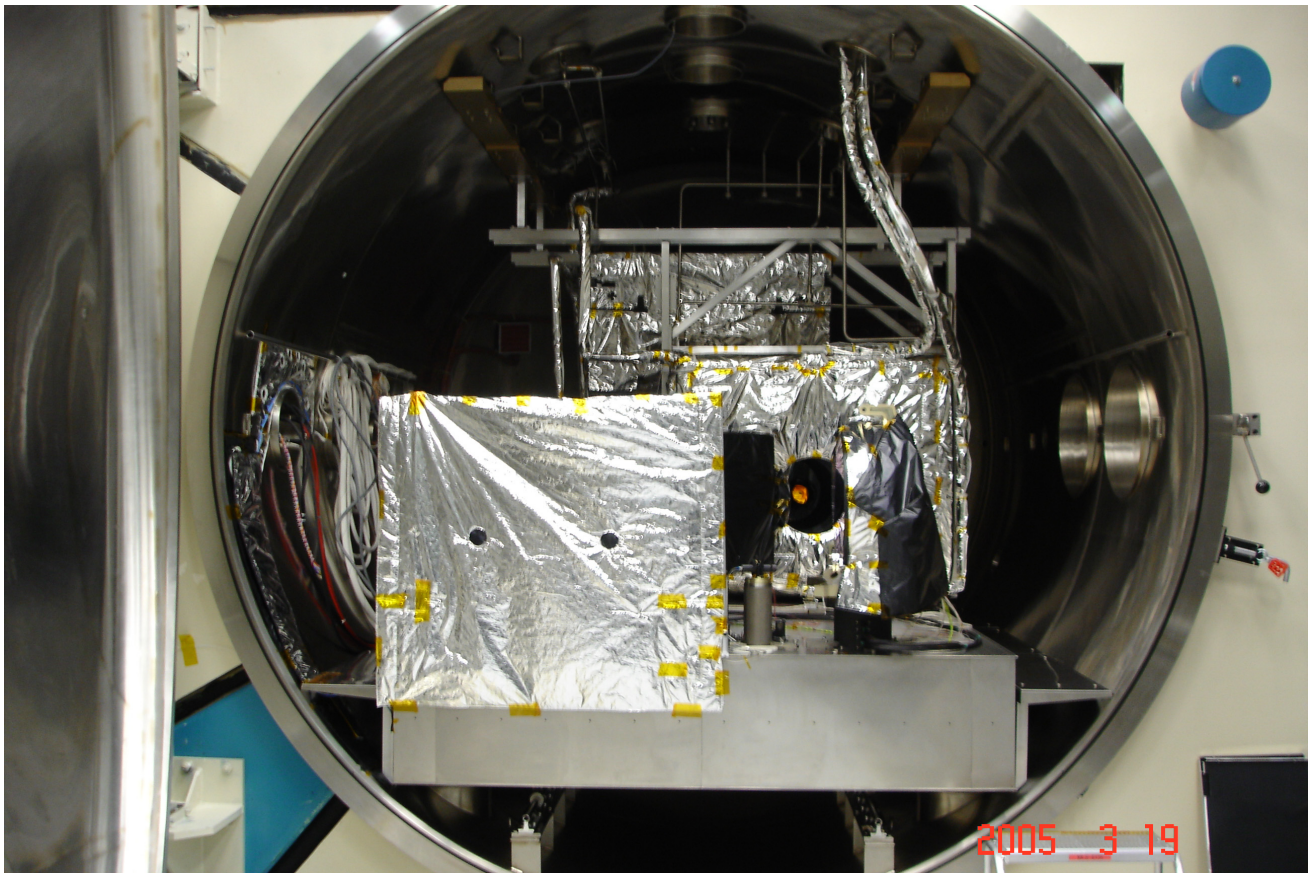


Figure 1 – The TOM3 testbed in the 3.3 meter vacuum chamber at JPL.

Figure 1 is a picture of the TOM3 hardware in the chamber that provides the vacuum necessary to obtain the required sub-nanometer stability. Figure 2 shows a schematic optical layout of the TOM3 experiment. TOM3 consists of the following major assemblies:

The Common-Path Heterodyne Interferometer (COPHI) is the main optical sensor, designed to measure changes in the optical wavefront phase over the pupil after reflection on the test articles.

The flight-like optical beam compressor assembly is the first test-article in this experiment. It is described in more details in section 3. It is used backward to expand the 50mm diameter COPHI metrology beam up to 350 mm in order to map the siderostat aperture.

The 500mm chopping/fold flat mirror is mounted on top of a motorized rotation stage that toggles between two positions. In the retro-mode position, the mirror is used as a reference while assessing the thermo-mechanical performance of the beam compressor. In the siderostat mode, it is used as a fold mirror that relays the expanded COPHI beam out of the compressor onto the siderostat.

The siderostat is SIM's starlight collecting aperture of the science interferometer. In the TOM3 experiment, it is the main test-article that retro-reflects the metrology beam back to the COPHI sensor. The flight-like siderostat consists of a 380 mm flat mirror with an embedded cube corner at the center. The siderostat is located inside a thermal shroud that simulates the on-orbit flight-like thermal environment.

The on-orbit thermal disturbance is mainly from the change in the relative position of the sun with respect to SIM. The typical SIM observation scenario will generate about 7 degrees of spacecraft motion every hour in order to slowly cover the entire sky. A relatively smaller thermal disturbance is from the change in the position of the siderostat relative to the rest of the instrument hardware due to the articulation of the siderostat. The siderostat will acquire light from stars anywhere in the 15 degrees field of regard. These two sources of thermal disturbances are emulated in TOM3 using the thermal shroud.

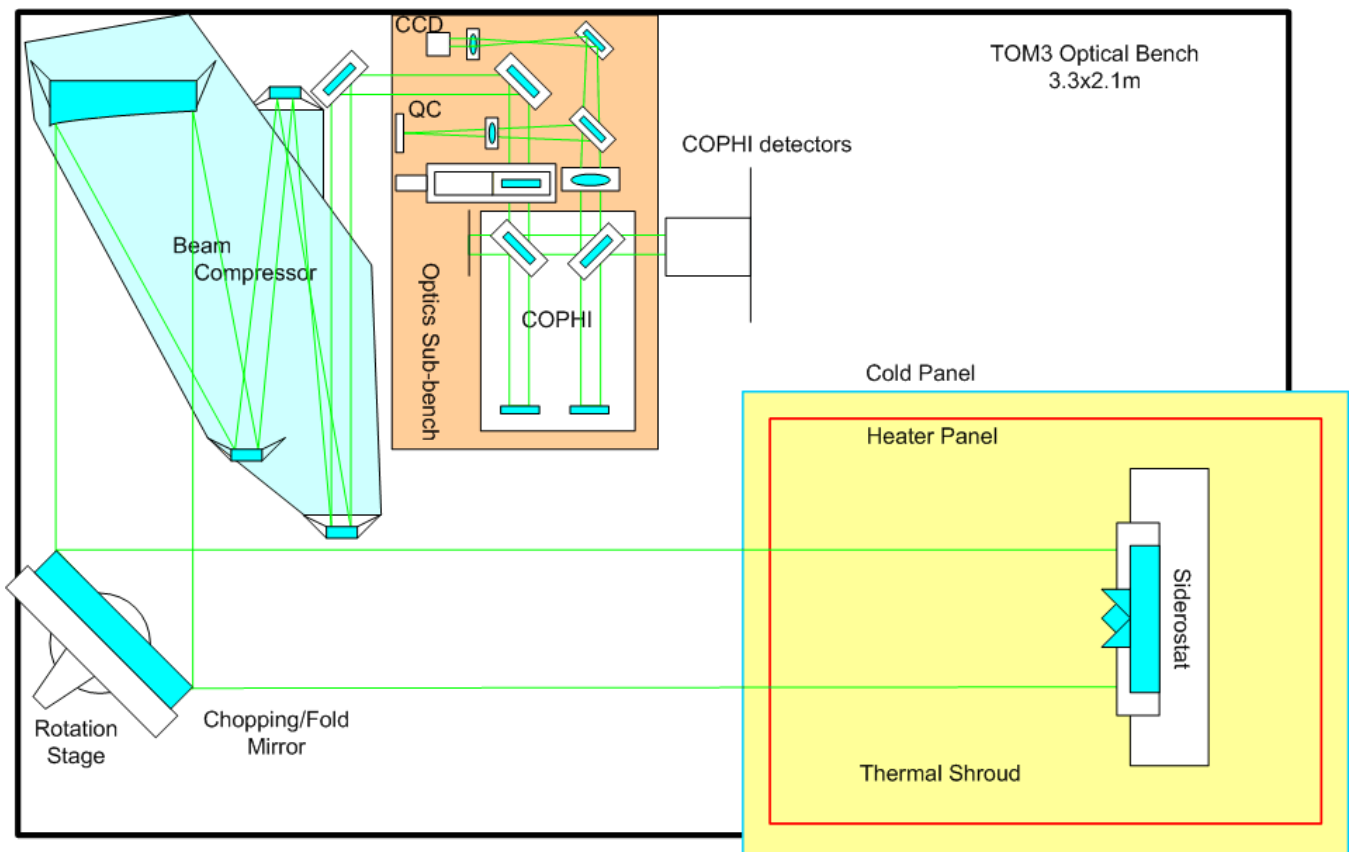


Figure 2 – TOM3 main optical layout inside the vacuum chamber

## 2. COMMON-PATH HETERODYNE INTERFEROMETER

COPHI uses standard heterodyne metrology techniques, but it has been modified in order to do precise relative metrology of various portions of the pupil. Details on the COPHI interferometer can be found in references [7] and [8]. Figure 3 illustrates the COPHI metrology in the vacuum chamber as well as the laser source outside of the vacuum chamber.

The coherent laser light from a 532 nm frequency-double Nd:Yag laser is split into two beams that we will be named in the rest of the paper "Local Oscillator" (LO) and "Measurement Beam" (MB). The frequency of these two laser beams is then shifted by respectively 80 and 80.01 MHz using acousto-opto-modulators (AOMs). Using a pair of single mode polarization-maintaining fibers designed for 532nm, the laser light is brought to the COPHI sub-bench in the vacuum chamber.

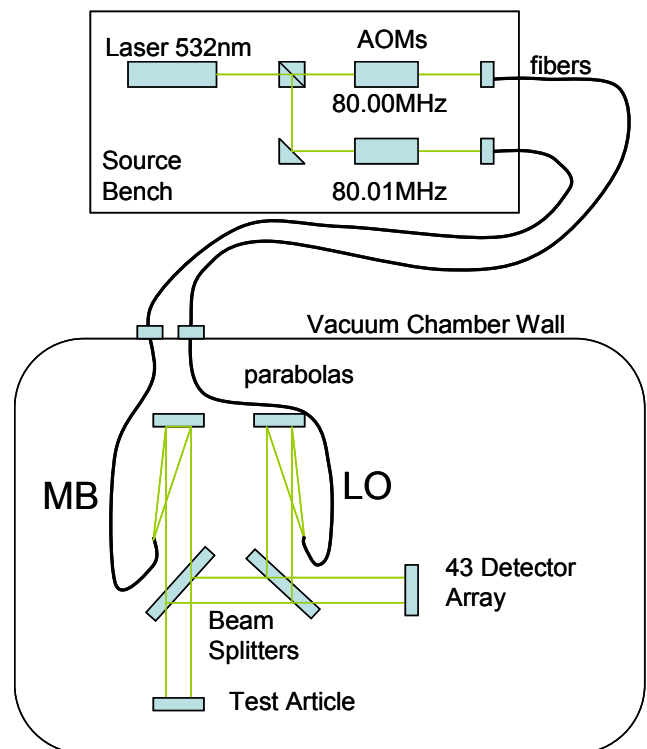


Figure 3 – COPHI detection

The light from the two fibers is collimated using off-axis parabolas. A pair of 50/50 beam splitter windows forms the main interferometer. Each of the beam splitters has a specific role. The measurement beam (MB) transmits through the first beam splitter window, propagates to the test article, retro-reflects and returns back to the same beam splitter. The light that reflects from that beam splitter window propagates to the second beam splitter window where it mixes and interferes with the local oscillator (LO) beam. Additional paths and reflections do not contribute to the metrology and are not displayed in Figure 3. In order to maintain required stability within the interferometer, the two parabolas and beam splitters are mounted on top of a Zerodur glass bench, which has a very low coefficient of thermal expansion..

The combined light is then collected by an array of 43 photo-detectors. The detectors are sampled in the pupil plane as shown in Figure 4. A 10 kHz sine wave signal, due to the interference of the 80 MHz MB signal with the 80.01 MHz LO signal, is observed at each detector. In a perfect optical system all detectors would produce 10 kHz sine waves in phase. In the real case, the aberration in the optical wavefront at the beam recombination produces relative phase offsets between the 10 kHz waves at the various detectors. This relative phase difference is measured very accurately by the COPHI electronics, providing a precise measurement of the aberration in the wavefront (or OPD change).

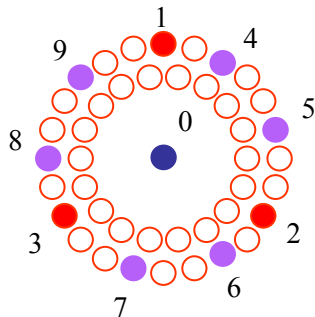


Figure 4 – Location of the 43 detectors within the pupil plane.

Figure 5 illustrates the COPHI electronics. Starting in the vacuum chamber, at the detector array, the 10kHz signal is amplified by the array of pre-amplifiers. To reduce the size of the COPHI readout electronics, the 43 signals are multiplexed. The electronics enable us to observe 10 detectors at a time, of which 4 are fixed and read continuously (detector 0 at the center of the array in Figure 4 and detectors 1, 2 and 3 in the outside at 120 degrees from each others) and 6 are selectable using the multiplexer.

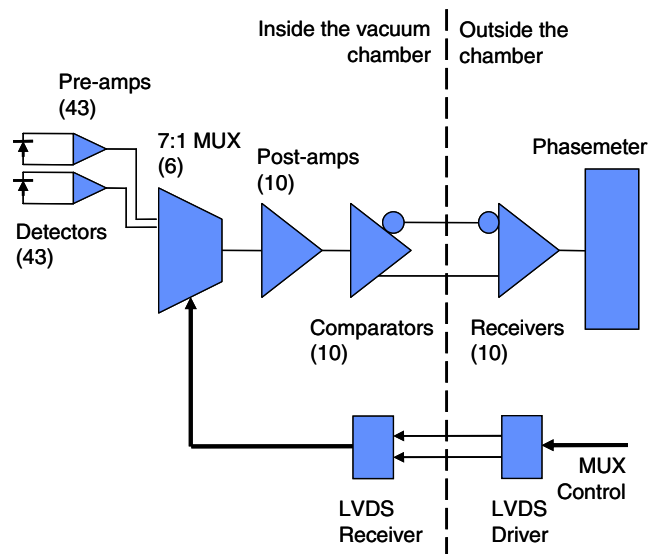


Figure 5 – COPHI Metrology Electronics

A custom VME board (phase meter) produces the precise relative phase measurement at every zero crossing of the 10kHz signal [9]. The relative phase detection uses a fast counter at 128MHz that starts on the reference signal and stops on the target signal. We have chosen to always use the signal produced by the central detector (in Figure 4) as the reference. The single measurement resolution<sup>3</sup> of the phase meter at 10kHz is approximately 40pm. However, the phase meter is capable of on-board averaging to obtain a much finer resolution. Sub-picometer resolution can be achieved after a few seconds of integration.

The test article under measurement with COPHI is one of the three following optics:

- A small 75mm diameter reference flat mirror, located right next to the COPHI interferometer, used for calibration of COPHI.
- The large 500mm diameter reference flat mirror, located in the expanded beam side of the compressor, used to monitor the thermal performance of the flight-like beam compressor.
- The flight-like 380mm diameter siderostat flat mirror, with an embedded cube-corner at its center, located in the expanded beam side of the compressor.

Finally, using the light from the other port of the main recombination beam splitter in the COPHI sub-bench, the pupil is imaged on a CCD camera (Figure 2) in order to achieve good system alignment prior to the start of each test.

<sup>3</sup> The instantaneous resolution of the phasemeter can be calculated from the ratio of the fast clock to the heterodyne frequency and from the metrology laser wavelength:

$$532\text{nm} * 10\text{kHz} / 128\text{MHz} = 0.041\text{nm} \sim 40\text{picometers.}$$

### 3. TEST ARTICLES

#### *Flight-like beam compressor*

SIM's optical beam compressor bench assembly is designed to receive optical starlight reflected from the siderostat. The compressor is a three-mirror anastigmat telescope design, with a flat fold mirror to make it compact. This light is compressed by a ratio of 7:1 (from 35cm entrance beam to a 5cm exit beam). The optical path is shown in Figure 6.

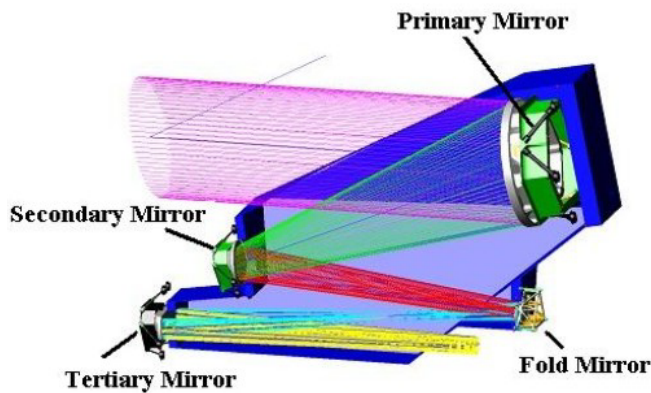


Figure 6 – Compressor bench optical path

The flight-like compressor tested in TOM3 consists of a large composite optical bench, built by ATK, which constrains four static mirror assemblies: the primary mirror, secondary mirror, fold mirror, and tertiary mirror. The composite panels form an egg-crate structure. The light-weighted mirrors, polished by Tinsley, were aligned by SSG Precision Optronics, Inc. Table 1 lists the major components of the assembly.

Table 1 – Flight-like compressor hardware list

Component	Function	Material
Compressor Bench	Low CTE metering support of the optics	M55J
M1 Mirror Glass	Receives 350mm diameter optical beam	ULE
M1 Mirror Mount	Supports M1 mirror glass	Invar
M2 Mirror Glass	Receives optical beam from M1	ULE
M2 Mirror Mount	Supports M2 mirror glass	Invar
Fold Mirror Glass	Receives optical beam from M2	ULE
Fold Mirror Mount	Supports Fold mirror glass	Invar
M3 Mirror Glass	Receives optical beam from Fold mirror	ULE
M3 Mirror Mount	Supports M3 mirror glass	Invar

The compressor bench was not located within the thermal shroud and was instead passively thermally controlled with Multi-Layer Insulator (MLI) blankets. The lack of thermal control made the bench susceptible to diurnal temperature changes in the chamber wall as well as soak changes from the presence of the cold liquid nitrogen shroud in the chamber. However, the resulting thermal environment turned out to be very similar to the expected beam compressor on-orbit thermal environment.

#### *Flight-like siderostat*

The primary test article is the flight-like siderostat shown in Figure 7. The siderostat optic consists of a 380 mm light-weighted ULE-glass flat mirror, built by Tinsley, with an embedded Zerodur cube corner at the center, built by Research Electro-Optics, Inc. Table 2 lists the major components of the assembly.

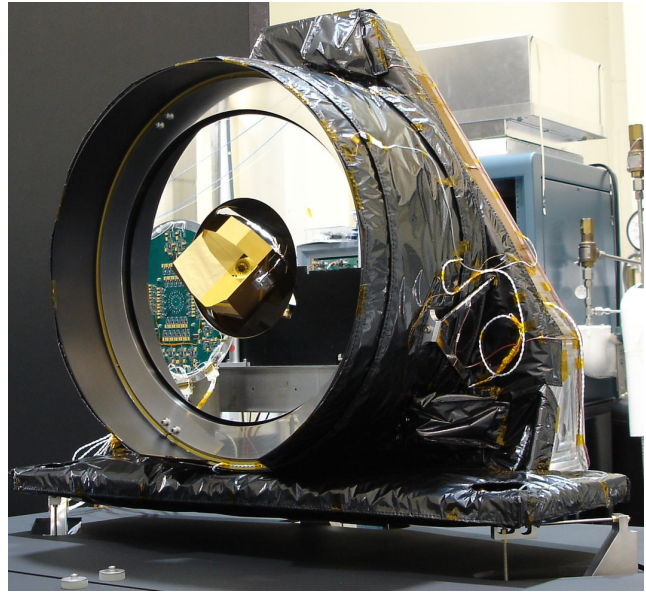


Figure 7 – Flight-like siderostat

The siderostat optic is thermally controlled by an aft thermal can (radiative enclosure surrounding the rear half of the mirror). A forward thermal can extends beyond the plane of the mirror face in order to reduce mirror lateral thermal gradients. A control Platinum Resistance Thermometer (PRT) on the aft thermal can controls seven heater patches wired in parallel. Heaters are driven by a Lakeshore 332 controller using a Proportional-Integral-Derivative (PID) heater control. Details of heater properties and their locations are shown in the next section.

Table 2 – Flight-like siderostat hardware list

Component	Function	Material
Siderostat Flat Mirror	380mm diameter reflecting surface	ULE
Bezel	Supports siderostat mirror	Super Invar
De-Space Monopods	Contains PZT actuators for alignment	Invar
De-Center Monopods	Holds bezel to support structure	Invar
Support Structure	Supports mirror assembly	Invar
Double Corner Cube	Sampled by SIM's metrology	Zerodur
DCC Post	Supports DCC	ULE
Aft Thermal Can	Mirror radiative thermal control	Aluminum
Forward Thermal Can	Reduces lateral thermal gradients	Aluminum
Thermal Can Bipods	Supports thermal can from structure	Titanium
Interface Bipods	Supports entire assembly from bench	Invar

Fine pointing of the siderostat is achieved with three PZT actuators connecting the siderostat support structure with the siderostat bezel. Coarse pointing actuation of the siderostat was not implemented for the TOM3 test. This omission is the primary difference between the TOM3 siderostat and the flight design. Instead of using a coarse

pointing actuator, the temperature field of the thermal enclosure is varied to simulate the changing thermal environment around the siderostat.

The siderostat support structure consists of two large Invar parts. The vertical part of the support fixture is controlled by a PID heater circuit consisting of 5 heater patches. The horizontal part of the support fixture is controlled by a PID heater circuit consisting of one heater patch. The entire mirror assembly is supported from the optical bench on three bipods with bases machined from invar and bipod legs made from stainless threaded rod. The bipods also provide thermal isolation for the siderostat.

The siderostat assembly is located inside the thermal shroud described in the next section. The shroud simulates flight-like boundary temperatures (190K to 250K) for the siderostat. The inside walls of the shroud assembly are actively controlled to ensure very stable boundary conditions.

#### 4. THERMAL SYSTEM

##### *Vacuum chamber*

The TOM3 testbed is installed inside a 3.3 meter vacuum chamber at the Jet Propulsion Laboratory. The chamber is equipped with mechanical roughing pumps as well as molecular turbo pumps for high vacuum. For thermal testing, it is important to have a high vacuum, as the thermal conduction through the remaining gas (mostly nitrogen) in the chamber at  $10^{-4}$  Torr pressures is high enough to add uncontrollable heat leak to the siderostat. This makes thermal model correlations much more difficult. During the TOM3 test, we maintained the vacuum chamber pressure near  $10^{-6}$  Torr level.

The 3.3x2.1 meter optical table is supported on air isolators, located outside the chamber, with thin-wall bellows feed-through to the platforms that contact the table. After fine adjustment, they provide mechanical isolation of the optical bench from the tank and the thermal shroud in six degrees of freedom. Additionally, all of the connections to the chamber required vibration isolation measures.

##### *Thermal Shroud*

The thermal shroud has a box configuration and consists of a dual panel construction (Figure 8). The goal of this construction was to provide a stable boundary temperature for the siderostat by attenuating any temperature fluctuations on the liquid nitrogen (LN<sub>2</sub>) panels by utilizing the thermal capacitance of the plates as well as the radiative

heat exchange between the plates. The stability requirement for the internal panels was +/- 0.5K/hr. Both sets of panels are 6mm thick and are painted with Aeroglaze Z-306 black paint. The outer shroud panels are cooled by means of LN<sub>2</sub> supply lines, vacuum brazed to one side. During the test, these lines are kept flooded to ensure as stable temperatures as possible.

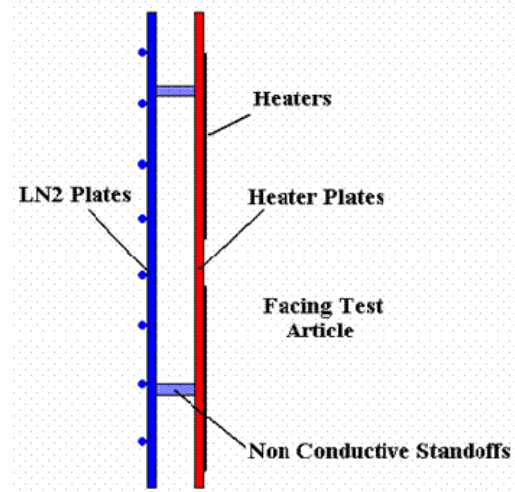


Figure 8 – Shroud dual panel construction

The internal panels are actively temperature controlled with Lakeshore PID temperature controllers to the desired set-points. Each side of the box has two independent heater panels. All of the panels are controlled on separate heater circuits so different set-points could be dialed in for each. Film heaters, providing at least 80% coverage for an even heat flux, are mounted to the inner panels. Very stable temperatures (+/- 10mK/hr) were achieved on the inner heater panels while the outer LN<sub>2</sub> panels were flooded with LN<sub>2</sub>. Ten of the twelve inner panels are conductively isolated from the outer panels by means of G10 standoffs. The two door inner panels however, are conductively coupled to the outer door panel by means of aluminum standoffs. The colder door panels simulate the open aperture boundary condition of a flight-like Collector Bay.

Most heater circuits used Lakeshore 332 temperature controllers to supply power. Heaters circuits requiring more power (heater plates, siderostat heater cans) used Agilent 6643A, 6644A, and 6654A power supplies in conjunction with a Lakeshore 332 temperature controller.

The thermal shroud can be operated to provide both steady state and transient conditions. The LN<sub>2</sub> panels are flooded at all times to minimize temperature instabilities. Transient temperature changes on the heater plates are induced to simulate the changes in temperature of the internal Collector Bay MLI during nominal spacecraft slew and Siderostat Mirror articulation in space.

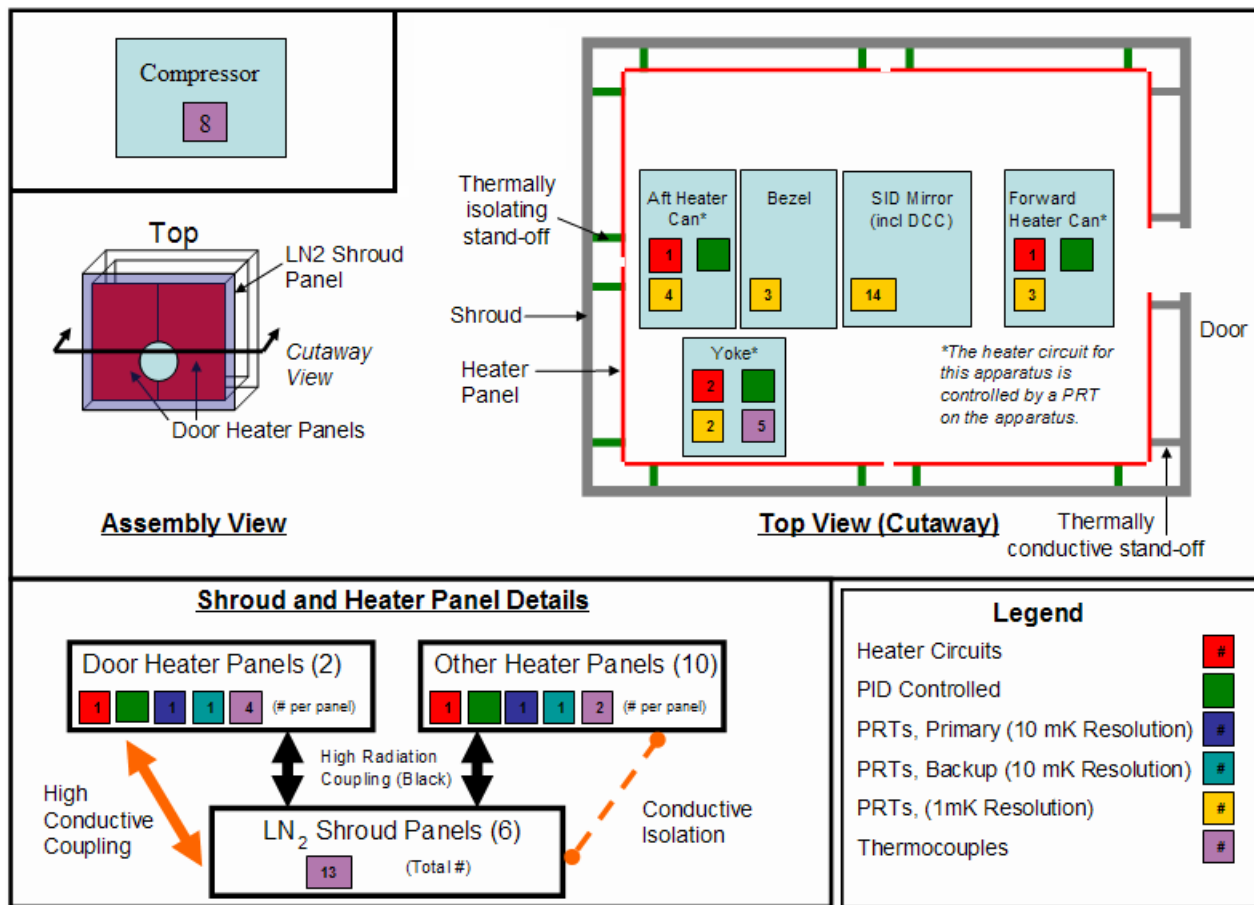


Figure 9 – Thermal instrumentation block diagram

### Thermal sensors

Forty eight thermocouples and 51 Platinum Resistance Thermometers (PRT) are used in this test. Figure 9 is a block diagram showing the number and type of temperature sensor/heaters located on each piece of hardware.

For areas where changes in temperature need to be accurately measured, 4-pin Lakeshore-111 PRT sensors with individual calibration curves (calibrated at 70 points over temperature range of 70K to 325K) are implemented. During testing, telemetry resolution was approximately +/-3mK. Heater control PRTs on the shroud heater panels, on the siderostat yoke, and on the siderostat thermal can heater circuits are monitored by Lakeshore 332 temperature controllers. The remaining PRTs which are mounted to the siderostat are monitored by a specialized milli-Kelvin Temperature Measurement System.

It was not possible to use a conductive epoxy such as Stycast to attach PRT to glass components due to the concern that it would locally degrade the glass low CTE. A deformation analysis was completed, confirming unacceptable glass deformations in the region of the PRT

epoxy weld. For this reason, all glass mounted PRT are installed using thermal grease and Kapton tape. On the thermal can and siderostat support structure, small holes are drilled into the hardware to receive the PRT bead.

Thermocouples are used where the precision and expense of PRT are not warranted. The standard 26 gage Type-E Chromel-Constantan thermocouples are mounted to the test article, to the thermal shroud panels and to the vacuum chamber. Each thermocouple has a 13mm by 19mm copper tab with P-389 acrylic adhesive and a 6.4 m long duplex wire lead with PFA Teflon insulation. In order to avoid thermocouples popping loose during the test, a strip of Kapton tape was applied to each tab for additional holding power. Aluminized Kapton tape is used in selected areas where there are low emittance requirements.

Thermocouple and PRT locations are selected where allowable flight temperature limits apply. Thermocouples and PRT are also placed at important hardware interfaces and in locations that would aid in analytical model correlation. Other thermocouples and PRT are placed to characterize special gradients.

### Milli-Kelvin temperature measurement system

TDAS (Thermal Data Acquisition System), a LabView based data acquisition system is used for this test. All data (time, date, temperature, power, voltage, and current) is monitored and automatically recorded at one-minute intervals. The Lab-View based system is interfaced with the Lakeshore 332 temperature controllers. PID heater control constants as well as control method (PID or constant power) could easily be toggled through the LabView interface.

Prior to the beginning of the test, the coefficients derived from the 70 point PRT calibration for each individual PRT were uploaded to the LabVIEW program. As the PRT resistance values get monitored by a Linear Research 700 (LR-700) system, the program applies the PRT specific coefficients to an equation to determine and display the appropriate temperature value.

The time constant associated with the LR-700 processing is dependent upon the filter internal to the LR-700; a 10 second filter was used in this application. Typically, 3 time constants were required in order to get quality data. The LR-700 system can measure resistance values to a resolution of approximately 0.1 milli-Ohms (about 0.25mK).

## 5. TEST RESULTS

### Science interferometer

SIM's science interferometer collecting optics consists of a siderostat followed by a beam compressor on each arm of the interferometer. This is simulated on TOM3 when the chopping mirror is in the siderostat position.

Figure 10 shows the temperatures measured inside the thermal shroud during a typical TOM3 test run. The shroud panel temperatures range from 95 K at the door panel that simulates cold space to 210 K at the top panel that simulates the MLI temperature of the instrument panel on the sunny side of the spacecraft. The siderostat and DCC temperatures are kept near ground room temperature (290 K) by the PID thermal control.

Figure 11 shows more details on the temperature measured on the thermal shroud side panels during the same test run. The one-hour-period variation of the temperature simulates the change in the thermal load on the siderostat as it would articulate to acquire stars in the sky. The slower 14-hour-period variation of the temperature simulates the change in the thermal load on the siderostat due to the spacecraft motion.

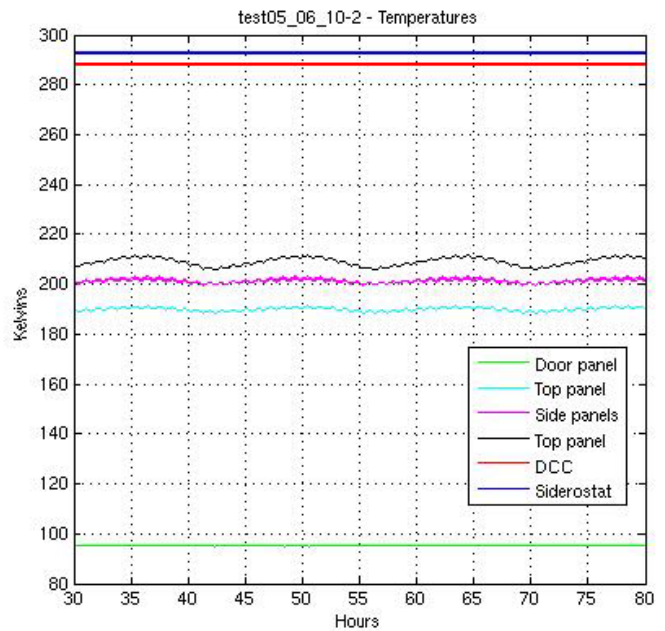


Figure 10 – Temperatures of the siderostat mirror, double corner-cube and shroud panels during a typical 50 hour run.

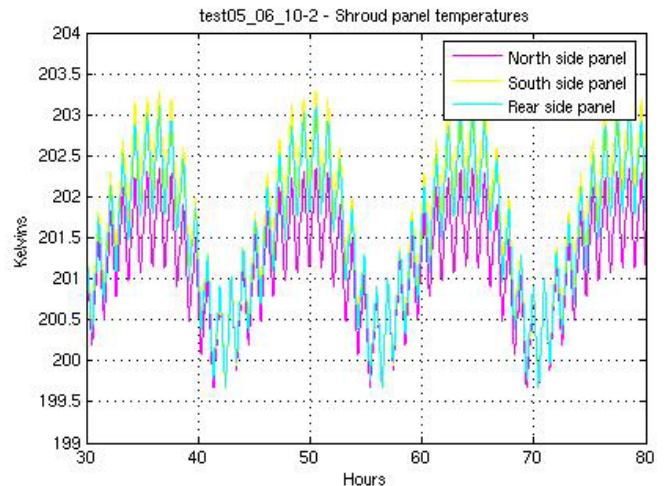


Figure 11 – Shroud temperature during the siderostat test. The Top panel temperature at 190 K, the Bottom panel temperature at 210 K and the Door panel at 95 K are not visible at this scale.

Figure 12 shows the temperature variation of the siderostat mirror surface and DCC. Although the shroud temperature is around 200 K, the mirror surface is kept at the required 293 K thanks to the siderostat thermal control. The DCC being more exposed to the shroud thermal load than the siderostat, its temperature is about 5 K cooler. The one-hour-period thermal excitation is not observable on the siderostat article optics. The 14-hour-period thermal excitation is significantly attenuated by the siderostat thermal control scheme, from about 2 K amplitude (in Figure 11) down to 50 mK at the siderostat surface and 25 mK at the DCC.

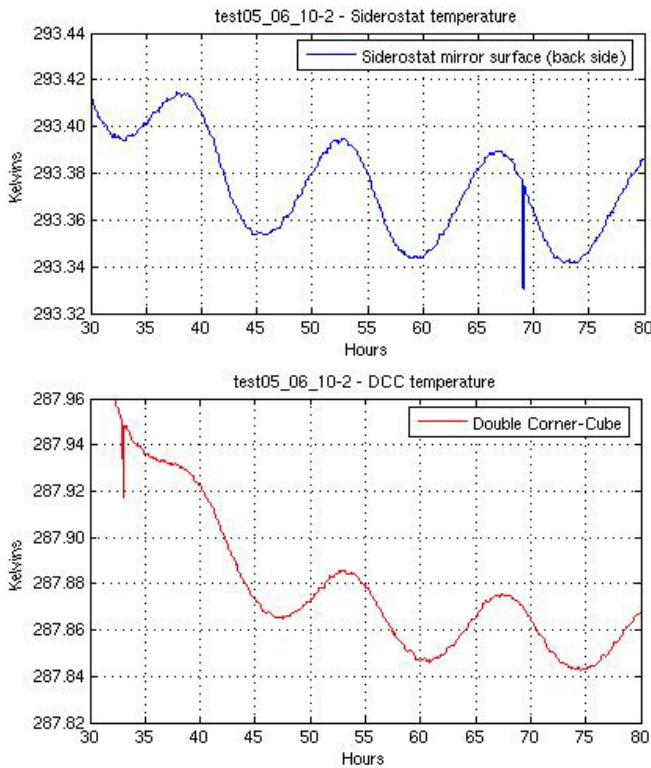


Figure 12 – Temperature variations on the siderostat and double corner-cube during the siderostat test.

Figure 13 shows the raw data from a typical TOM3 run. COPHI metrology data was recorded continuously at 10Hz for about 17 hours. The metric of interest is the optical path difference between the central detector that samples the cube corner at the center of the siderostat optic and the average of nine detectors, uniformly located in the outer ring, after reflection from the mirror portion of the siderostat. The constant value (around 60 nanometers) in the data is due to the residual defocus aberration of the beam compressor (one tenth of a wave at 633 nm). Note a slow downward drift mostly produced by the diurnal cycle of the temperature outside of the vacuum chamber. Slow fluctuations of a few 100 picometers over several hours were traced back to thermal instability of the optical fibers.

Figure 14 shows the final post-processed result (143 picometers) for the same data run after applying SIM's wide angle processing [5]. In this observation scenario, the linear drift of the instrument is removed every hour, by repeating the same observation at the beginning and the end of the hour. Within each hour, the data is integrated for 30 seconds at a time to mimic the integration on SIM's target stars.

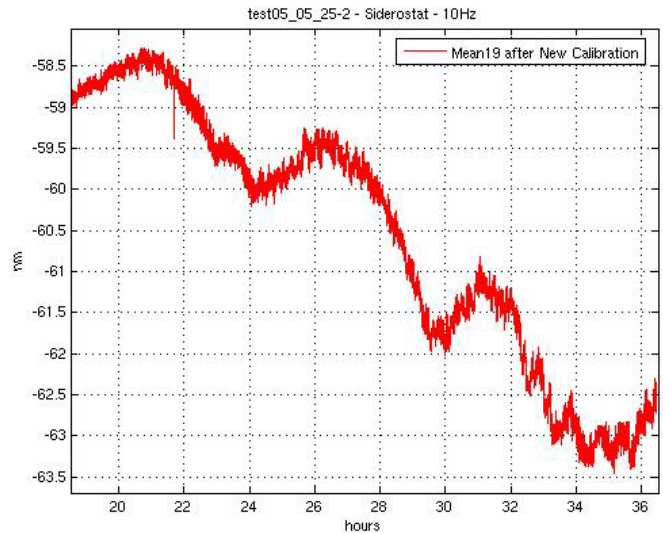


Figure 13 – COPHI measurement of the siderostat, optical path difference of the average of 9 detectors relative to the central detector, in nanometers.

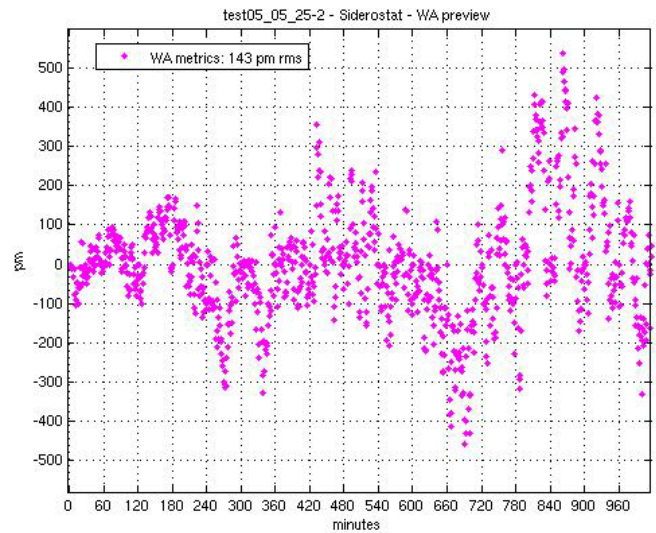


Figure 14 – Data from Figure 13, processed with SIM's wide angle observation scenario, in picometers.

Figure 15 shows the final post-processed result (10.6 picometers) for the Figure 13 data run after applying SIM's narrow angle processing [4]. In short, in this observation scenario, twelve chops between a target and a reference stars are averaged together. The 30 second integration time and the 90 second chop period help in reducing the sensitivity to fast noise (faster than a few seconds) as well as very slow fluctuations (slower than a few milli-Hertz) and drift of the instrument.

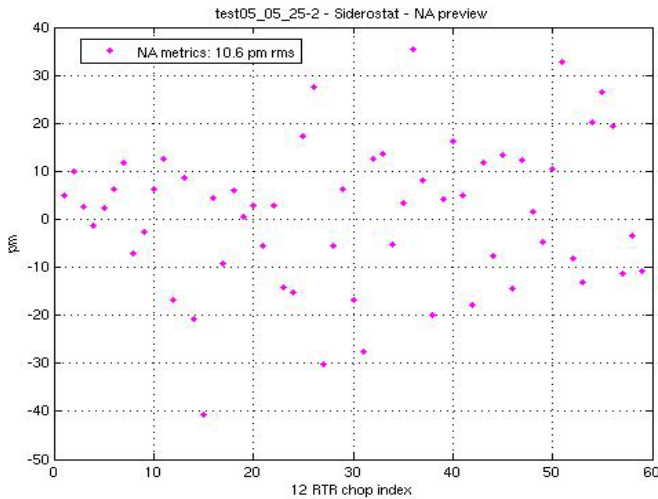


Figure 15 – Data from Figure 13, processed with SIM’s narrow angle observation scenario, in picometers.

### Guide interferometer

SIM’s guide interferometer collecting optics consists only of a beam compressor on each arm of the interferometer. This is simulated on TOM3 when the chopping mirror is in the retro-mode position.

Figure 16 shows the data from a TOM3 test run, characterizing the compressor thermal response. COPHI metrology data was recorded simultaneously with thermal data for almost 50 hours. Again, the metric of interest is the OPD between the central detector and the average of nine detectors, uniformly located in the outer ring, after reflection from the large reference flat on the expanded beam side of the beam compressor.

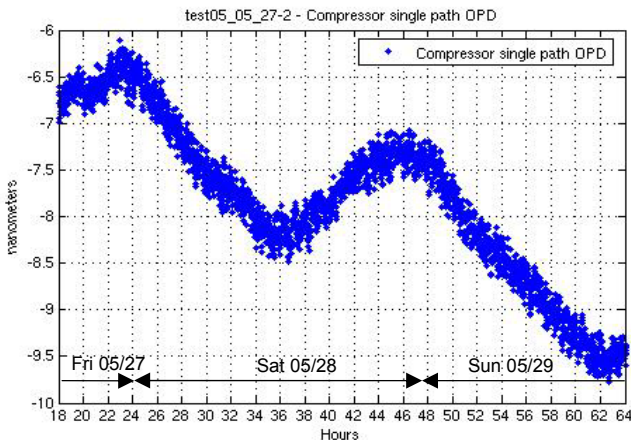


Figure 16 – COPHI metrology data from the beam compressor, in nanometers.

Figure 17 shows the temperature for five thermal sensors mounted on the beam compressor, three on the composite bench, one on the primary mirror glass and the last one on

the secondary mirror glass. One can observe a static thermal gradient within the compressor and a soak temperature change.

Comparing the optical data from Figure 16 and the thermal data from Figure 17, one can see an obvious correlation between the thermal excitation and the optical response. The slow downward drift and the diurnal cycle of the temperature suggest a 4 nanometers per Kelvin linear thermo-opto-mechanical sensitivity of the compressor (single path). The thermal structural model predicts a slightly higher sensitivity of 5 nm/K [10].

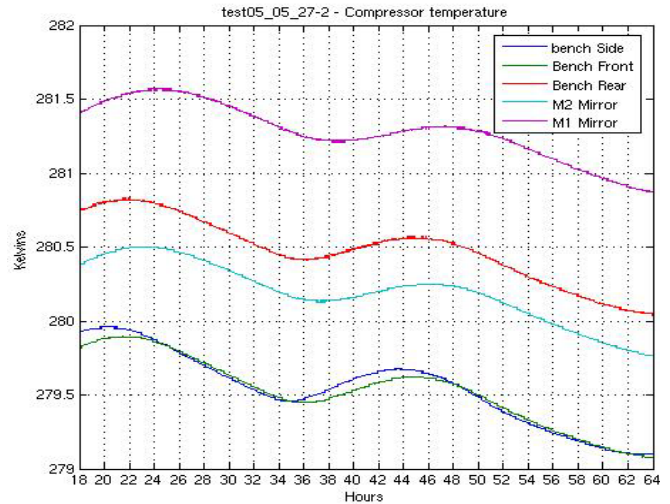


Figure 17 – Temperature of the beam compressor

### Performance summary

Table 3 summarizes about 500 hours of thermal testing on the TOM3 testbed. The results are sorted by type of test. In the Guide interferometer tests, only the beam compressor is tested. In the Science interferometer tests, both the beam compressor and the siderostat are tested. Also, during the science test, the temperature in the thermal shroud is varied in a flight-like manner to simulate either the Inboard collector bay at about 200K or the Outboard bay at about 190K.

Table 3 – TOM3 test summary

Test	Baseline Requirement	Run Time	Test Result
Guide Narrow Angle Either Bay	10.8 pm	108 hours	5.4 pm
Guide Wide Angle Either Bay	280 pm	148 hours	99 pm
Science Narrow Angle Inboard Bay	22.2 pm	56 hours	9.5 pm
Science Wide Angle Inboard Bay	570 pm	40 hours	198 pm
Science Narrow Angle Outboard Bay	22.2 pm	56 hours	8.7 pm
Science Wide Angle Outboard Bay	570 pm	85 hours	204 pm

The baseline requirement allocated from SIM's error budget is shown in the first column. Note that the tests meet all the requirements with some margin. SIM is also carrying a goal performance budget, about 4 times tighter than baseline error budget. The test results do not meet that goal performance. However, further testing showed that the current TOM3 performance is limited by the stability of the optical fibers that inject the light in the COPHI interferometer. Thermally "overdrive" tests confirmed that the test article thermal performance is significantly better than the results indicate.

## 6. CONCLUSION

We have discussed the TOM3 testbed developed to assess the thermo-opto-mechanical stability of optical assembly such as SIM's siderostat and telescope in flight-like thermal conditions. Although limited by the metrology sensor noise, test results show that optical wavefront stability of SIM's optical assembly is compatible with single micro-arcsecond astrometry.

## ACKNOWLEDGEMENTS

The research described in this publication was performed at the Jet Propulsion Laboratory of the California Institute of Technology, under contract with the National Aeronautics and Space Administration. The authors would like to thank Edouard Schmidlin, Jim Moore, Shonte Wright, Yuanming Liu and the TOM3 team for their contribution to the success of the experiment.

## REFERENCES

- [1] J. Marr, "Space Interferometry Mission (SIM) overview and current status," *SPIE conference on Interferometry in Space*, vol. 4852, 2002.
- [2] R. A. Laskin, "SIM technology development overview -light at the end of the tunnel", *SPIE conference on Interferometry in Space*, vol. 4852, 2002.
- [3] R. Goullioud, O.S. Alvarez-Salazar, and B. Nemati, "Dim star fringe stabilization demonstration using pathlength feed-forward on the SIM Testbed 3 (STB3)", *SPIE Conference on Interferometry in Space*, vol. 4852, 2002.
- [4] R. Goullioud and T. J. Shen, "SIM astrometric demonstration at 24 Picometers on the MAM Testbed", *IEEE Aerospace Conference, Big Sky, MT*, 2004.

[5] R. Goullioud, T. J. Shen, and J. H. Catanzarite, "Wide angle astrometric demonstration on the Micro-Arcsecond Metrology testbed for the Space Interferometry Mission", *International Conference on Space Optics, Toulouse, France*, 2004.

[6] F. G. Dekens, "Kite: status of the external metrology testbed for SIM", *SPIE Conference on New Frontiers in Stellar Interferometry*, vol. 5491, 2004.

[7] F. Zhao, J.E. Logan, S. Shaklan, and M. Shao, "A common-path, multi-channel heterodyne laser interferometer for sub-nanometer surface metrology", *SPIE International Conference on Optical Engineering for Sensing and Nanotechnology*, vol. 3740, pp. 642-645, 1999.

[8] F. Zhao, "Demonstration of sub-Angstrom cyclic non-linearity using wavefront-division sampling with a commonpath laser heterodyne interferometer", *American Society for Precision Engineering annual meeting*, Crystal city, VA, 2001.

[9] P. Halverson, D. R. Johnson, A. Kuhnert, S. B. Shaklan, and R. E. Spero, "A multi-channel averaging phase meter for picometer precision laser metrology", *SPIE International Conference on Optical Engineering for Sensing and Nanotechnology*, vol. 3740, 1999.

[10] C. A. Lindensmith, H. C. Briggs, Y. Beregovski, V. A. Feria, R. Goullioud, Y. Gursel, I. Hahn, G. Kinsella, M. Orzewalla, C. Phillips, "Development and validation of high precision thermal, mechanical, and optical models for the Space Interferometry Mission", *IEEE Aerospace Conference, Big Sky, MT*, 2006.

## BIOGRAPHY

**Dr. Renaud Goullioud** has an electronics engineering degree from the Institute of Chemistry and Physics of Lyon (France) and a Ph. D. in micro-electronics from the National Institute of Applied Sciences of Lyon. He has been working at Jet Propulsion Lab on the Space Interferometry Mission as system engineer since 1997. He has developed several system testbeds related to the SIM mission. He has demonstrated path length feed-forward control among three interferometers on the SIM Testbed and picometer-level sensing on SIM-like interferometer in the Micro-Arcsecond Metrology testbed. In October 2004, he took responsibility of Thermo-Opto-Mechanical testbed.

